Proceedings of IMECE'03
2003 ASME International Mechanical Engineering Congress
Washington, D.C., November 15–21, 2003

IMECE2003-41105

APPLICATION OF LASER SCATTERING ON DETECTION OF SUBSURFACE DAMAGE IN SILICON WAFERS

J.M. Zhang
Kansas State University
Department of Industrial and Manufacturing Systems Engineering
Manhattan, Kansas 66506
U.S.A.
1-785-532-3736
jzh9595@ksu.edu

J.G. Sun
Argonne National Laboratory
Energy Technology Division
Argonne, Illinois 60439
U.S.A.
1-630-252-5169
sun@anl.gov

Z.J. Pei
Kansas State University
Department of Industrial and Manufacturing Systems Engineering
Manhattan, Kansas 66506
U.S.A.
1-785-532-3436
1-785-532-3738 (fax)
zpei@ksu.edu

ABSTRACT

Silicon is widely used in semiconductor industry. Over 90% of all semiconductor devices are manufactured upon silicon substrates (wafers). Many manufacturing processes are needed for the wafer preparation. In order to ensure high quality silicon wafers, the damaged layer induced by each manufacturing process must be reduced or eliminated by its subsequent processes. So, it is critical to assess subsurface damage (SSD). As a nondestructive measurement method, laser scattering is preliminarily applied to measure SSD in silicon wafers. Optical transmission properties of silicon wafers are measured first to make sure that silicon wafers have the appropriate optical transmission properties for laser scattering. Photomicrographs and scatter images are obtained on sample wafers with different depth of subsurface damage. The correlation between photomicrographs and scatter images is discussed. The results from this study show that laser scattering can potentially be applied to measure subsurface damage across whole silicon wafers.

KEYWORDS

Laser scattering; Material removal; Semiconductor materials; Silicon; Subsurface damage

1. INTRODUCTION

Silicon is the primary semiconductor material used to fabricate microchips. After crystal growth, the single-crystal ingot will undergo a series of processes to be transformed into silicon wafers that meet stringent specifications (thickness, flatness, strength, etc).

The traditional manufacturing processes are as follows [1, 2]: (1) Slicing (ID sawing or wire sawing): to slice the silicon ingot into wafers of thin disk shape. Currently wire sawing is mostly used because of its high efficiency. (2) Edge contour grinding: The edges of sliced wafers, which are sharp and fragile, need to be shaped robust. (3) Flattening (lapping or grinding): Slicing will not produce perfectly flat wafers, especially wire sawing will induce "waviness" into the wafer surface [3]. During lapping, the front and back surfaces of the wafer simultaneously undergo an abrasive treatment, so "waviness" is efficiently removed. (4) Etching: After lapping and grinding, the wafers are very flat, but directly underneath the surface, there is a mechanically damaged layer. Etching can remove this mechanically damaged layer without introducing further mechanical damage. (5) Polishing: This process is both mechanical and chemical. It gives the surface the required flatness and smoothness. (6) Cleaning: to remove the particles from the wafer surface.

However, some of these manufacturing processes (such as lapping and grinding) will lead to the introduction of surface and subsurface damage. In order to avoid failures in the final device production, this damaged layer must be removed by the subsequent processes. Therefore, there is a critical need to measure the depth of subsurface damage caused by these manufacturing processes.

There are many methods applicable to assess subsurface damage in silicon wafers. Some methods are destructive, meaning that the wafers will be destroyed during measurements. For example, in cross-sectional microscopy method, the samples are cleaved from the whole wafer, sanded, polished and etched. After these preparations, measurements are performed [1]. Some other destructive methods need to remove specific layers from the surface, such as etching method [4], step polishing [5], etc. Compared with destructive methods, nondestructive methods have many advantages. The sample wafers do not need any preparations, and after measurements the samples can still be used for further development. There is reported research on photoluminescence [6] and micro-Raman spectroscopy [7, 8]. The former technique is for subsurface lattice disorder; the latter one is for phase transformation. Both of them measure subsurface damage (SSD) on the smaller scale. A nondestructive method to measure SSD on a larger scale - subsurface microcracks (from several μm to tens of μm deep) is desired.

Optical techniques have been widely applied for nondestructive measurements of surface roughness and subsurface damage. Especially laser scattering technique has been successfully used to detect surface and near-surface defects in ceramics [9, 10]. It has the potential to scan the whole wafer within tens of minutes, and detect the damage of various depths across the whole wafer. This is a big advantage over other methods (such as cross-sectional microscopy) that can only reveal SSD information at specific areas on the wafer instead of the whole wafer.

This paper presents the results of a study on the application of laser scattering on SSD measurement in silicon wafers. It is organized into five sections. The first section is this introduction. In section 2, the background theory of laser scattering is described. Section 3 presents the experimental conditions and procedures. The experimental results will be presented and discussed in section 4. And some conclusions are drawn in section 5.

2. BACKGROUND THEORY OF LASER SCATTERING

When a light is incident on a surface between two media, part of the light is reflected from the surface, and part is refracted. As shown in Fig. 1, P_i is the incident light, P_r the reflected light from the surface, P_r' the refracted light, θ_i the incident angle, θ_r the reflection angle. If the surface is specular (perfectly smooth and reflective), the incident angle and the reflection angle will be numerically equal, which is called "specular" reflection. Otherwise, it is called "diffuse" reflection or scattering [11, 12].

Several optical scattering techniques have been successfully used for nondestructive evaluation and measurement of surface topography. The first approach is total integrated scatter (TIS), originally developed by H. Davies [13]. As shown in Fig. 2, the total intensity of the diffusely scattered light is measured by the detector. TIS is the ratio of this quantity to the total intensity of reflected radiation (specular plus diffuse). So TIS is shown to be related to the surface roughness parameter R_q (R_q represents the standard deviation of the profile about the mean line, defined by Eq. (1):

$$R_q = (L^{-1} \int_0^L y^2(x)dx)^{1/2} \quad (1)$$

where x is the distance along the surface, $y(x)$ defines the height of the surface profile about the mean line, and L is the sampling length). However, this method is practical only for very smooth surfaces with $R_q << \lambda$ (wavelength of the light) [14, 15].

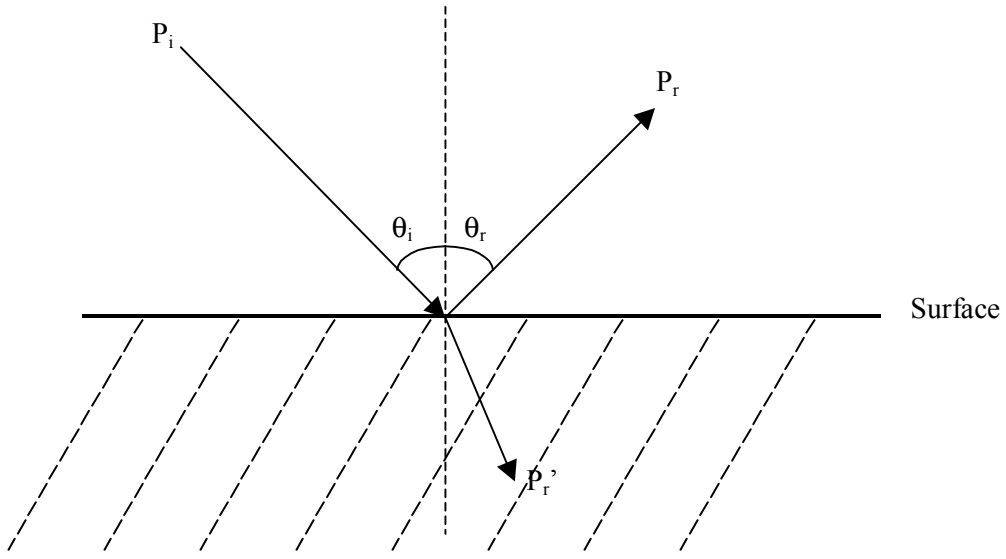

Fig. 1. Definition of scattering.

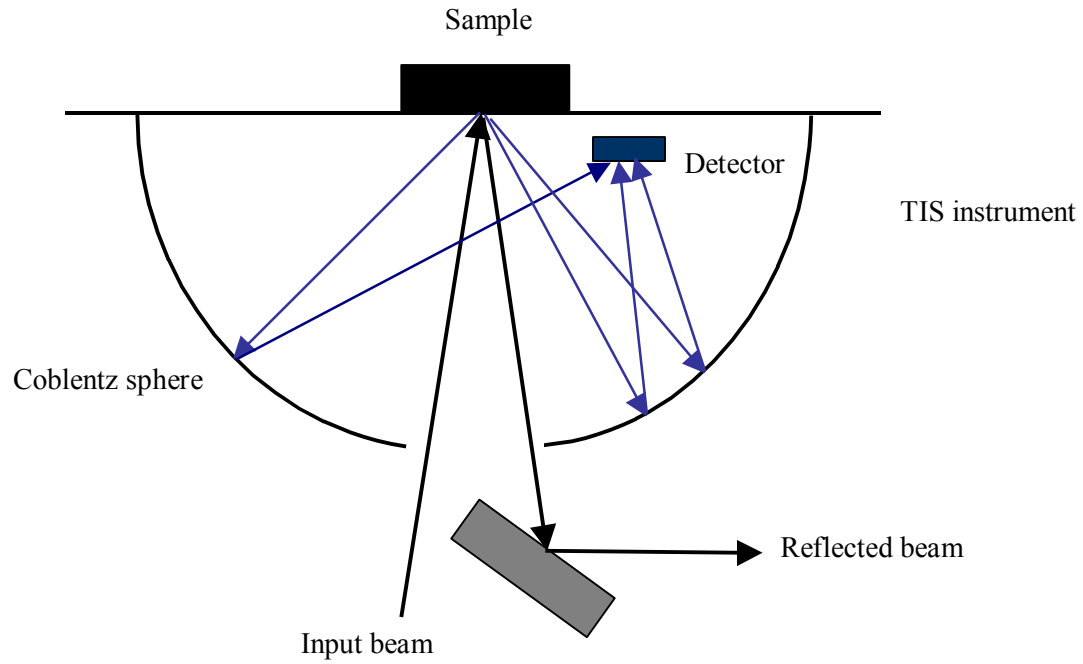

Fig. 2. Illustration of TIS.

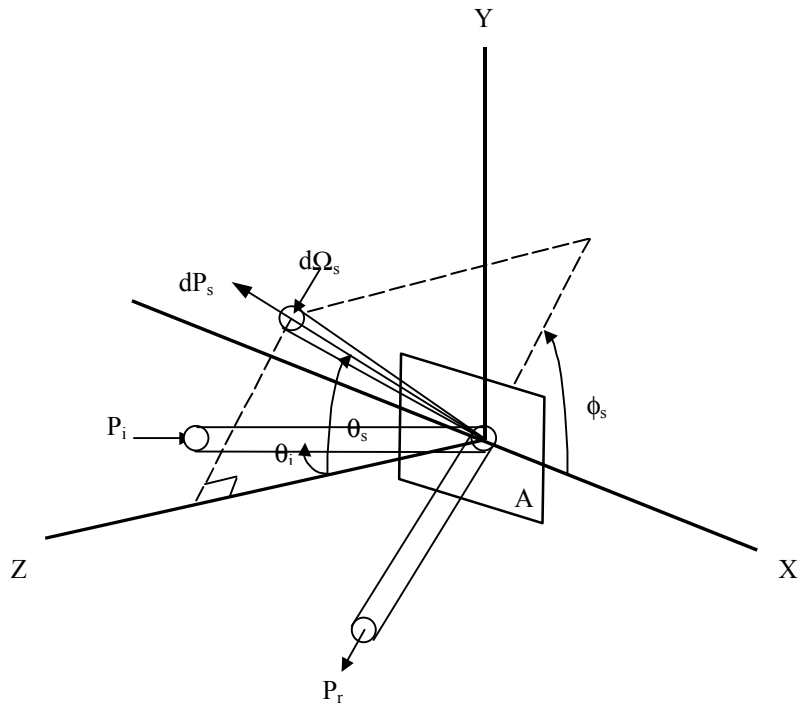

Fig. 3. Geometry for definition of BSDF.

The second technique to measure surface roughness is bidirectional scatter distribution function (BSDF). BSDF is defined as "the surface radiance divided by the incident surface irradiance." The surface radiance is the light intensity scattered through the scatter angle per unit illuminated surface area. The incident surface radiance is the light intensity incident on the surface per unit illuminated surface area. As shown in Fig. 3, BSDF is calculated by:

$$BSDF = \frac{P_s/\Omega_s}{P_i Cos\theta_s} \quad (2)$$

where P_i is the incident light, P_s the scattered light, P_r the specularly reflected light, Ω_s the illuminated surface area, θ_i the incident angle, θ_s the scatter angle, and ϕ_s the angle between the scatter direction and X axis (the scatter direction is determined by P_s and Z axis) [15]. A uniformly illuminated nontransparent isotropic surface is assumed for this technique, so BSDF is not applicable for the anisotropic surface [15, 16].

The third technique commonly used for surface analysis is the speckle contrast measurement. When the coherent light illuminates the rough surface, the reflected beam accounts for

part of the random patterns of bright and dark regions known as "speckle". The speckle pattern is created by the interference of wavelets scattered from points of different heights within the illuminated area (as shown in Fig. 4, where v is the angle of illumination and h the height of the roughness) [17]. In the speckle contrast measurement, the average contrast, defined as the normalized standard deviation of intensity variations at the observed surface, has a strong, linear correlation with the surface roughness parameter R_a [18, 19]. Roughness average R_a, the most widely used surface parameter, represents the average deviation of a surface profile about its mean line, defined as:

$$R_a = L^{-1} \int_0^L |y(x)| dx \tag{3}$$

where x, $y(x)$ and L have the same meanings as in Eq. (1) [14].

The three optical scattering methods described above are generally adequate for surface roughness measurements, but they are not suitable to assess subsurface damage. However, polarization property can be properly used to separate the combined effects of surface and subsurface. As shown in Fig. 5, where P_i is the incident light, P_r the specularly reflected light, P_s the scattered light, P_t the transmitted light, θ_i the incident angle, θ_s the scatter angle, $\theta_{i'}$ the principal angle, and ϕ_s the angle between the scatter direction and X axis. Each light beam has two perpendicular components (S and P) in the plain normal to the light propagation direction. For a relatively smooth surface, the polarization of the surface scattered/reflected light will only be changed mildly from that of the illuminating beam. But for the subsurface, multiple interactions occur between the light and material grain boundaries or microstructural discontinuities (such as subsurface defects), therefore completely randomizing the polarization of the scattered light [15, 20]. By properly selecting the source and detector polarization, the subsurface effects can be separated from the surface effects.

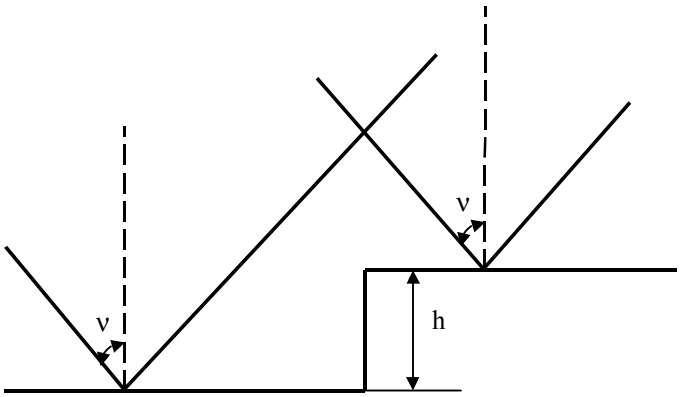

Fig. 4. Difference caused by surface roughness.

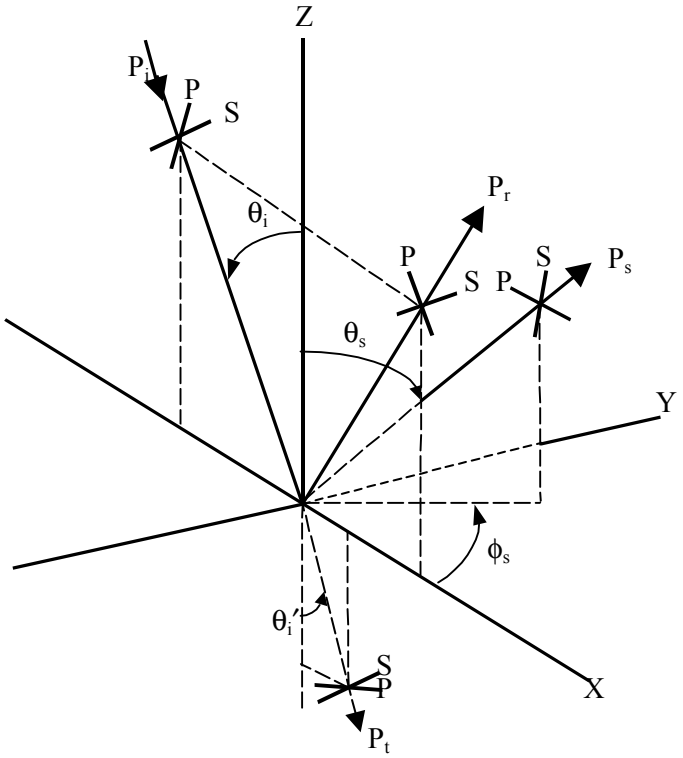

Fig. 5. Polarization of light.

3. EXPERIMENTAL CONDITIONS AND PROCEDURES

3.1 Measurements of Optical Transmission Properties

When the light is incident on the surface of a material, it can penetrate beneath the surface for a certain distance known as "skin depth" because of the finite absorption of the material. Any material has a characteristic "skin depth", as a function of optical frequency [9, 15]. Not all the materials are suitable for laser scattering measurement. For metals, the "skin depth" is only a few nanometers at most for visible wavelengths, thus scattering can be considered to emanate entirely from the surface. For silicon-nitride ceramics, the "skin depth" was found to be from tens to hundreds of microns [10], so laser scattering can be applied to measure SSD within that depth range. For silicon wafers, the optical transmission properties should be measured as the first and necessary step of this study.

An integrating sphere is used for the measurements of optical transmission properties (as shown in Fig. 6). Before fixing the sample wafer, the original light intensity is measured by the optical detector. After the sample is put on the fixture, the transmitted light intensity is measured. The percentage of transmission is the ratio of the transmitted light intensity and the original light intensity. Using different wavelengths and samples with different thickness, the optical transmission properties are obtained.

Seven silicon wafers with different thickness (100 μm, 150 μm, 200 μm, 250 μm, 300 μm, 350 μm, and 400 μm) are used as the experimental samples. All of these sample wafers are single crystal silicon wafers of 200 mm in diameter with (100) plane as major surface.

3.2 Laser Scattering Experiments

The three sample wafers for laser scattering experiments have the same diameter and orientation as the ones used in the preceding experiment, but with different depths of subsurface damage created by surface grinding. It is reported that depth of subsurface damage on ground silicon wafers is approximately equal to half of the diamond grit size of the grinding wheel [1, 21, 22]. As shown in Fig. 7, these three wafers are first coarse-ground by a grinding wheel with #320 mesh diamond size to different target thickness, and then fine-ground by a grinding wheel with #2000 mesh diamond size to a same final target thickness. Since these three wafers have different coarse-grinding target thickness and the same fine-grinding target thickness, the removal of fine grinding on these wafers are different (shown in Table 1). It is assumed that the coarse grinding wheel will produce SSD depth of 25 μm approximately, and the fine grinding wheel will produce SSD depth of 4 μm approximately. Therefore it is expected that the deepest SSD is in wafer A, and the lowest SSD is in wafer C. Furthermore, it is noted that wafer B and C have the same surface roughness, but different SSD depth.

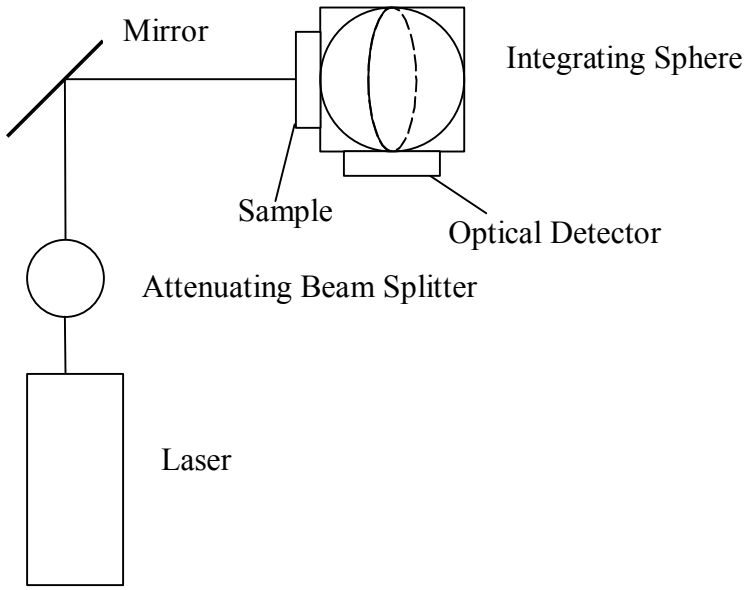

Fig. 6. Optical transmission properties measurement system.

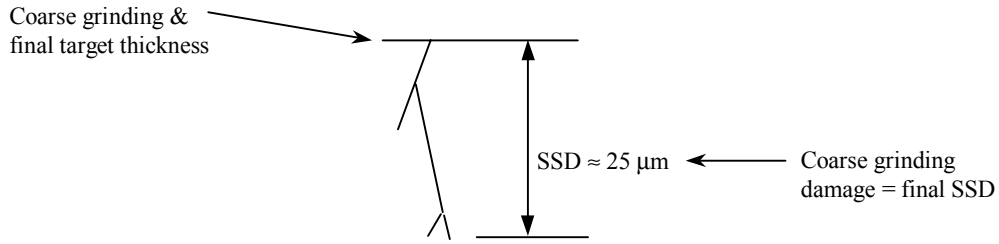

Wafer A: SSD ≈ 25 μm

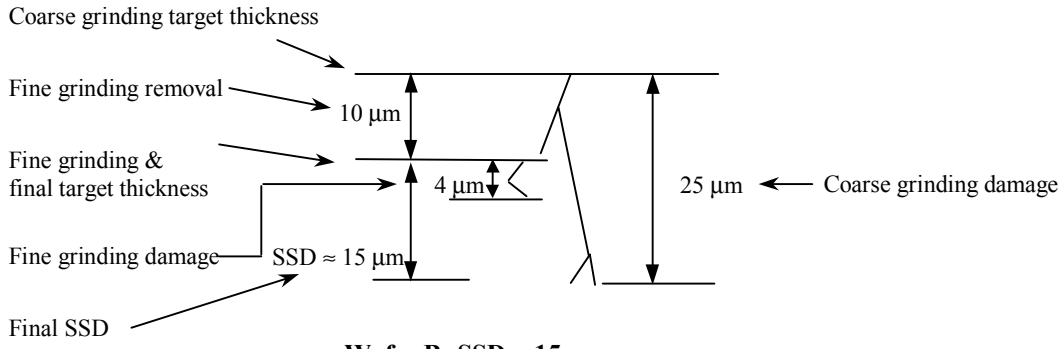

Wafer B: SSD ≈ 15 μm

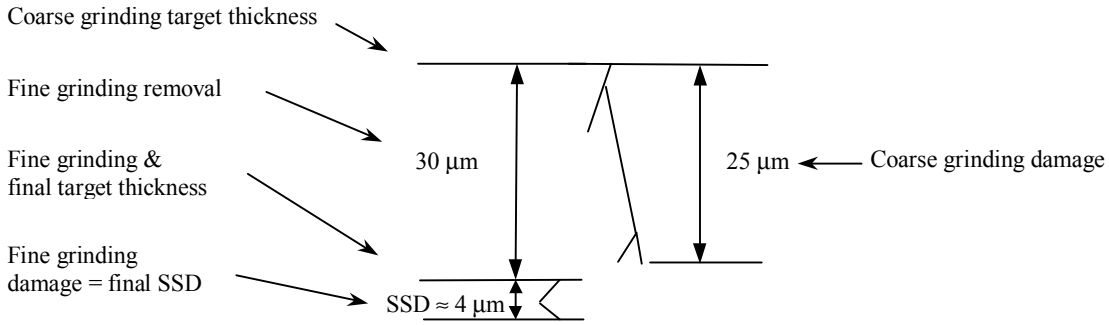

Wafer C: SSD ≈ 4 μm

Fig. 7. Different SSD depths of wafer A, B, & C.

Table 1. Fine grinding conditions used to prepare the sample wafers

Sample wafer	Fine grinding removal
Wafer A	0 μm
Wafer B	10 μm
Wafer C	30 μm

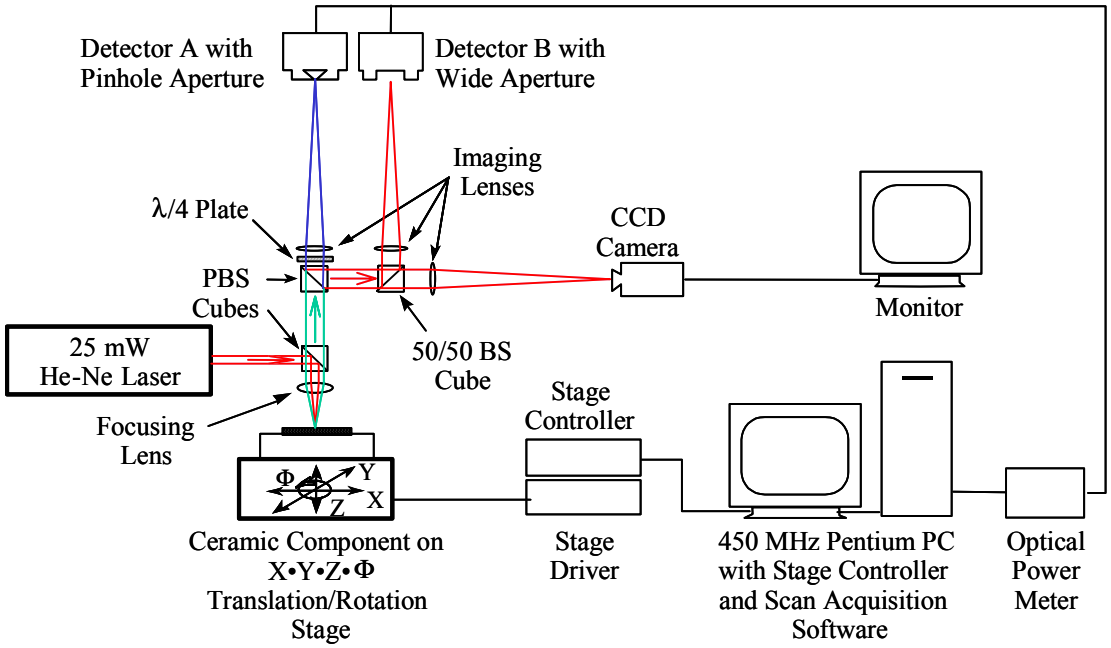

Fig. 8. Illustration of laser scattering system.

Table 2. Set-up parameters in laser scattering system

Parameter	Value
Image size	1.3 mm × 2.4 mm
Stage step size	5 μm
Incident angle	90 °
Depth of focus	0 mm

The experimental arrangement of laser scattering system is illustrated in Fig. 8 and the set-up parameters are listed in Table 2. Laser scanning is performed at the same location and area on each sample wafer. Two laser sources are available, a He-Ne laser at λ = 633 nm (Model 127, Spectra-physics Inc., Mountain View, CA, USA), and a Ti: sapphire tunable laser with a wavelength tuning range from 700 to 1000 nm (Model 3900S, Spectra-physics Inc., Mountain View, CA, USA). The vertically polarized laser beam is directed through a polarizing beam-splitter (PBS) cube and focused onto the specimen surface. Light scattered/reflected from this surface will not undergo change in polarization unless the surface is extremely rough; therefore, all surface-scattered light will be reflected in the PBS and directed back toward the laser. However, any light scattered from the subsurface material undergoes several reflections and refractions at grain boundaries and microstructural discontinuities (cracks), so it becomes completely diffused. Half of the subsurface-scattered light will be reflected in the PBS and directed back to the laser, the other half will be transmitted by the PBS into the detection train. The horizontally polarized back-scattered light that passes through the surface-illuminating PBS enters into the second PBS. Then it is directed through a quarter-wave (λ/4) plate, imaged by a positive lens onto a polished stainless steel pinhole aperture, and recorded by Detector A. Only the light scattered from the subsurface directly beneath the incident spot passes through the aperture and onto Detector A. The remaining light scattered from the area around the illuminating spot is reflected back through the lens and λ/4 plate. In this case, its polarization has been rotated to vertical, and it is reflected by the detecting PBS and directed to a 50/50 beam splitter. One side of this splitter is imaged by a positive lens onto Detector B, while the other side is imaged onto a CCD (Charge-Coupled Device) array to monitor the scattering pattern.

During the experiment, the sample is scanned in x-y directions and the detected signals are measured as the scattered light intensity in the unit of watt and processed to compose 2D scatter images of the scanned region.

3.3 Micrograph of Sample Wafers

After the sample wafers undergo the laser scattering experiments, they are observed under an optical microscope. The microscopy is performed at the same location as scanned and the photomicrograph is obtained.

4. RESULTS AND DISCUSSIONS

4.1 Optical Transmission Properties of Silicon Wafers

The optical transmission properties of silicon wafers are presented in Fig. 9. Figure 9(a) shows the optical transmission properties as the function of wavelength. The wafer thickness is 100 μm. When the wavelength increases, the percentage of transmission also increases, meaning that the light penetrates deeper into the silicon wafer. Therefore, using a longer wavelength, the deeper damage can be detected. Figure 9(b) is a plot of transmission versus thickness, at wavelength of 850 nm. It shows that the relationship between thickness (from 100 μm to 300 μm) and *Ln (% transmission)* (the logarithm of the

percentage of transmission to base *e* where *e* is 2.718) is almost linear. The data shown in Fig. 9 indicates that optical penetration from tens to more than 100 microns can be achieved for silicon wafers using wavelengths between 633 to 950 nm. From this test, it is concluded that silicon wafers have the appropriate optical transmission properties for laser scattering technique.

4.2 Correlation Between Photomicrographs and Laser Images

Figure 10 shows the photomicrograph and laser scatter images obtained at wavelengths of 633 nm, 850 nm, and 950 nm on the ground surface of wafer A. The grinding marks (lines) are seen on the surface photomicrograph in Fig. 10(a). The grinding-induced subsurface damage is shown in the scatter images in Figs. 10(b)~(d), where the white spots and lines represent subsurface regions with excessive scattered light due to machining damage. The correlation between white spots or white lines and subsurface damage can be found in Sun et al. [10]. The depth of subsurface damage may be assessed from these scans of different light wavelengths. Because the detected signal comes from all scattered light within the depth of light penetration which increases with the wavelength (refer to Fig. 9), short wavelengths can only detect shallow damage while longer wavelengths should detect both shallow and deep damage. The subsurface damage can be seen clearly from scatter images at all wavelengths, indicating that the subsurface damage is relatively deep. However, a correlation between the scatter image and SSD depth is yet to be determined.

Figure 11 shows the photomicrograph and laser scatter images obtained on the ground surface of wafer B. The photomicrograph shows only fine grinding marks that are approximately vertical in the image (see Fig. 11(a)). The scatter images obtained at wavelengths of 633 nm and 850 nm show some damage (excessive light scatter) along the fine grinding direction, though the scatter intensity is weak. However, all scatter images in Fig. 11(b)~(d) show damages at lower-left corner along an inclined direction approximately 30° from the vertical. This damage is not shown on the surface (see Fig. 11(a)) and apparently deep and severe. Many lower-intensity (or darker) lines and spots are also observed in the scatter images of higher wavelengths (Fig. 11(c)~(d)). The nature of this phenomenon is not well understood at present.

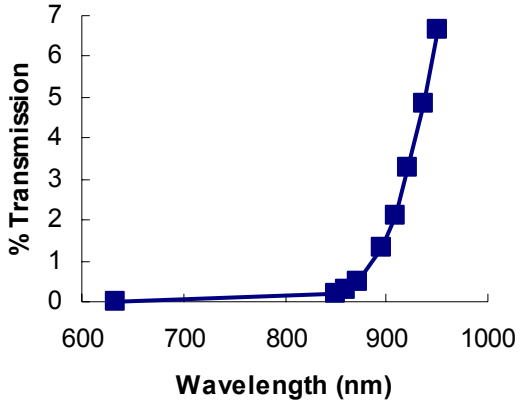

(a)

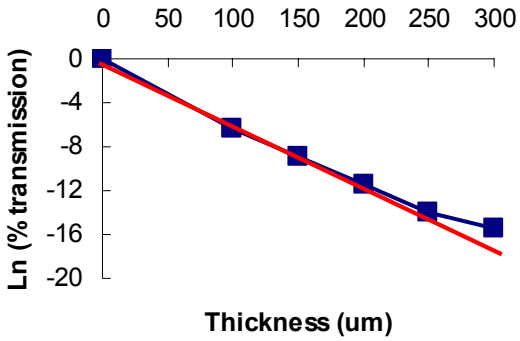

(b)

Fig. 9. Optical transmission properties of silicon wafers.

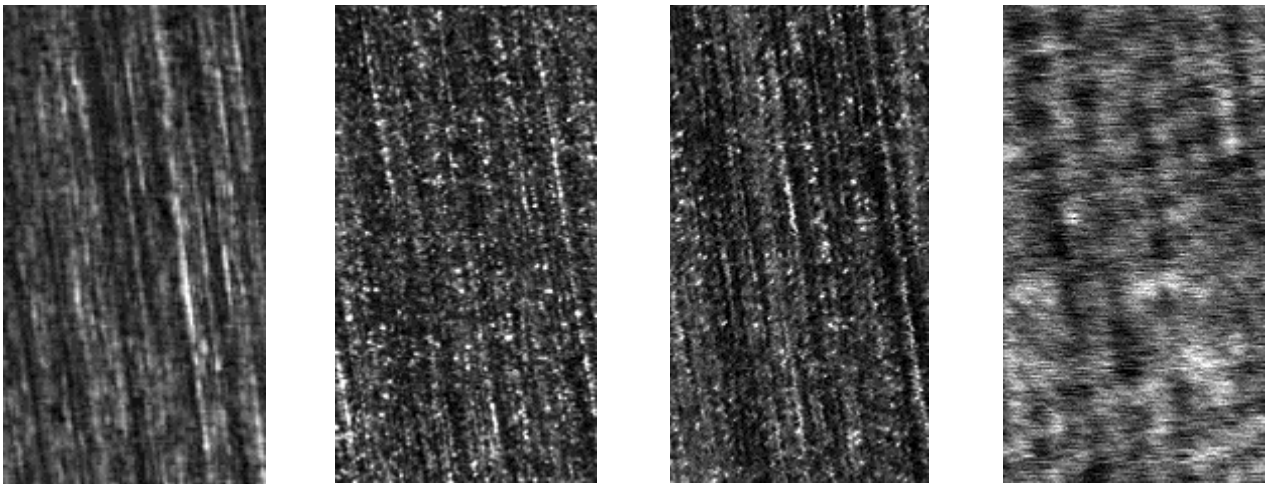

(a) Photomicrograph (b) Sum-image at 633 nm (c) Sum-image at 850 nm (d) Sum-image at 950 nm

Fig. 10. Results on wafer A.

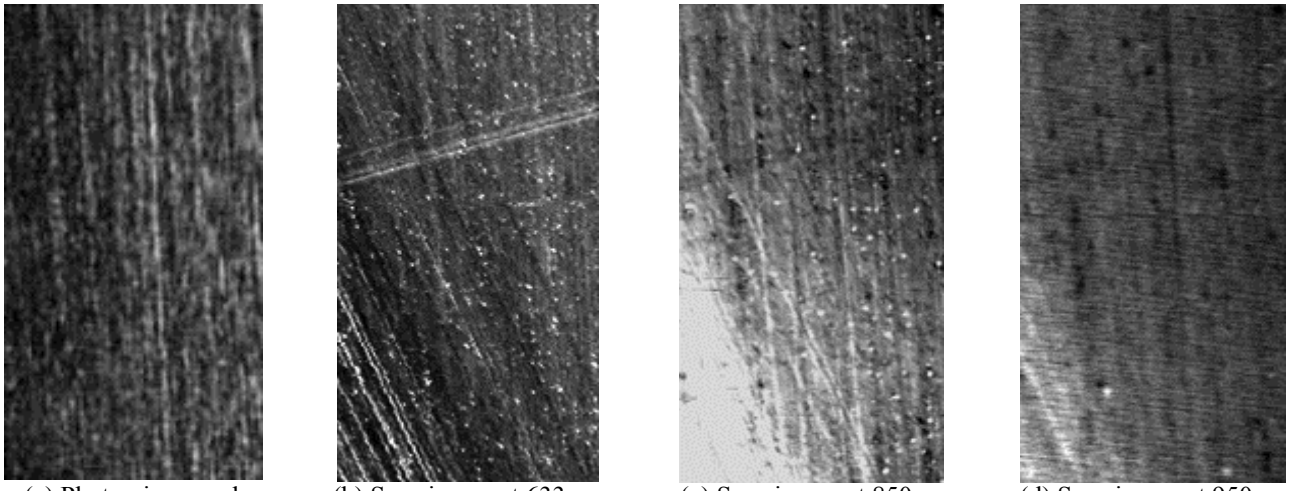

(a) Photomicrograph (b) Sum-image at 633 nm (c) Sum-image at 850 nm (d) Sum-image at 950 nm

Fig. 11. Results on wafer B.

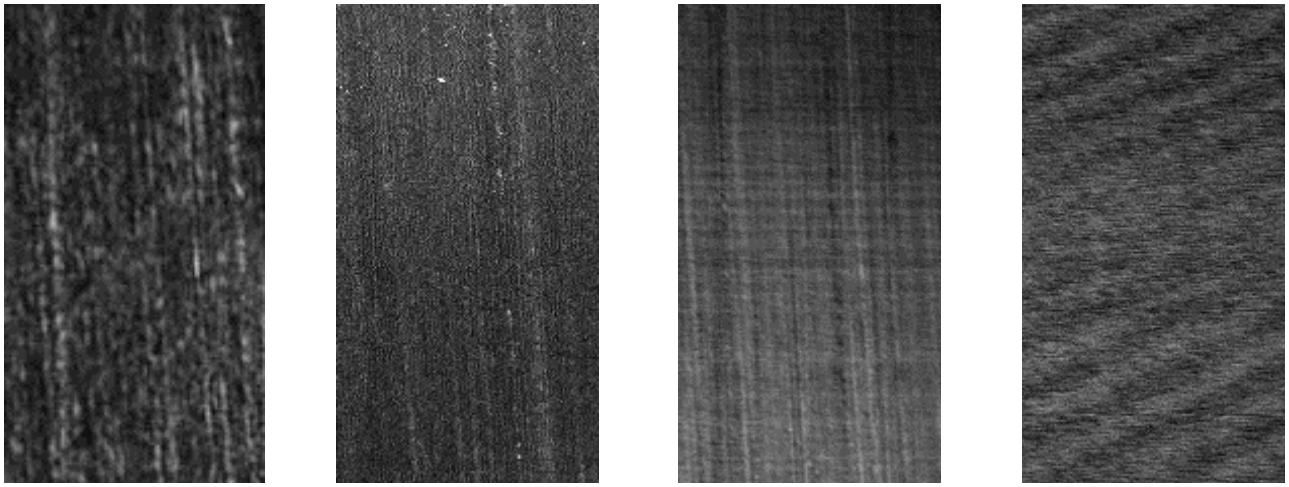

(a) Photomicrograph (b) Sum-image at 633 nm (c) Sum-image at 850 nm (d) Sum-image at 950 nm

Fig. 12. Results on wafer C.

Figure 12 shows the photomicrograph and laser scatter images obtained on the ground surface of wafer C. It is believed that fine grinding has removed all the damage caused by the initial coarse grinding. Again, the fine grinding marks are visible in the photomicrograph (Fig. 12(a)). However, there is minimal subsurface damage shown in Figs. 12(b)~(d). In Fig. 12(d), the scatter image at wavelength of 950 nm, there appears an interference pattern that is not understood at present.

As discussed in Section 3.2, wafer B and C are ground by the same coarse and fine grinding wheels but different fine grinding removal, therefore have the same surface roughness but different depth of subsurface damage. The same surface roughness can be seen from their photomicrographs (see Fig. 11(a) and Fig. 12(a)). Their scatter images are very different (see Fig. 11(b)~(d) and Fig. 12(b)~(d)). This indicates that the features captured by laser scatter images are not caused by surface roughness, but indeed associated with SSD.

4.3 Characteristic Attributes

In addition to the laser scatter images, some characteristic attributes can be calculated from the measurements of the scattered light intensity recorded by Detector A and B, such as maximum, range, and standard deviation, which seem to correlate to SSD depth in silicon wafers. The detailed discussions on these characteristic attributes have been published elsewhere [23].

5. CONCLUSIONS

Encouraging results have been obtained from a preliminary study of applying laser scattering technique on SSD measurement in silicon wafers. Three tests performed are measurements of optical transmission properties, laser scattering experiments, and taking micrography pictures on the sample wafers. The conclusions are:

(1) Silicon wafers have the appropriate optical transmission properties for laser scattering.
(2) Laser scattering technique can reveal the information of subsurface region.
(3) Shallow damage can be detected with short wavelength while deep damage can be seen with longer wavelength.
(4) Laser scattering can potentially be an efficient and nondestructive method to exam the whole wafers for subsurface damage evaluation.

ACKNOWLEDGEMENTS

Financial support was provided by the Advanced Manufacturing Institute at Kansas State University. The authors would like to thank Dr. Jeri Ikeda at Saint-Gobain Abrasives, Inc. and Mr. Salman Kassir at Strasbaugh, Inc. for providing the samples of ground silicon wafers.

REFERENCES

[1] Pei, Z.J., Billingsley, S.R., and Miura, S., 1999, "Grinding-induced subsurface cracks in silicon wafers," International Journal of Machine Tools and Manufacture, **39**, No.7, pp. 1103-1116.

[2] Quirk, M., and Serda, J., 2000, *Semiconductor Manufacturing Technology*, Prentice-Hall, Upper Saddle River, New Jersey.

[3] Pei, Z.J., and Fisher, G., 2001, "Surface grinding in silicon wafer manufacturing," Transactions of The North American Manufacturing Research Institution of SME, **29**, pp. 279-286.

[4] Tonshoff, H.K., Schmieden, W.V., Inasake, I., Konig, W., and Spur, G., 1990, "Abrasive machining of silicon," CIRP Annals – Manufacturing Technology, **39**, No. 2, pp. 621-630.

[5] Stephens, A.E., 1986, "Technique for measuring the depth and distribution of damage in silicon slices," Extended Abstract: Electrochemical Society Meeting, Boston, MA.

[6] Lucca, D. A., Hamby, D. W., Klopfstein, M. J., Cantwell, G., Wetteland, C. J., Tesmer, J. R., and Nastasi, M., 2001, "Effects of polishing on the photoluminescence of single crystal ZnO," CIRP Annals - Manufacturing Technology, **50**, No. 1, pp. 397-400.

[7] Kailer, A., Gogotsi, Y. G., and Nickel, K. G., 1997, "Use of hardness indentation coupled with micro-Raman spectroscopy in high-pressure materials research," Materials Research Society Symposium – Proc., Proceedings of the 1997 MRS Fall Meeting, pp. 225-230.

[8] Gogotsi, Y., Baek, C., and Kirscht, F., 1999, "Raman microspectroscopy study of processing-induced phase transformations and residual stress in silicon," Semiconductor Science and Technology, **14**, No. 10, pp. 936-944.

[9] Steckenrider, J.S., and Ellingson, W.A., 1994, "Surface and subsurface defect detection in Si_3N_4 components by laser scattering," Review of Progress in Quantitative Nondestructive Evaluation, **13**, pp. 1645-1651.

[10] Sun, J.G., Ellingson, W.A., Stechenrider, J.S., and Ahuja, S., 1999, *Application of optical scattering methods to detect damage in ceramics, Machining of Ceramics and Composites*, edited by S. Jahanmir, M. Ramulu and P. Koshy, Marcel Dekker, New York.

[11] Meyer-Arendt, J.R., 1989, *Introduction to classical & Modern Optics*, Prentice Hall, Englewood Cliffs, New Jersey.

[12] Neilson, W.A., Knott, T.A., and Carhart, P.W., 1961, *Webster's new international dictionary of the English language*, G. & C. Merriam Co., Springfield, MA.

[13] Davies, H., 1954, "The reflection of electromagnetic waves from a rough surface," Proceedings of the Institute of Electrical Engineers, **101**, pp. 209.

[14] Vorburger, T.V., and Teague, E.C., 1981, "Optical techniques for on-line measurement of surface topography," Precision Engineering, **3**, No. 2, pp. 61-83.

[15] Stover, J.C., 1990, *Optical Scattering Measurement and Analysis*, McGraw-Hill, New York.

[16] Nicodemus, F.E., Richmond, J.C., Hsia, J.J., Ginsberg, I.W., and Limperis, T., 1977, "Geometric considerations and nomenclature for reflectance," NBS Monograph 160, U.S. Dept. of Commerce, Washington, DC.

[17] Persson, U., 1992, "Real time measurement of surface roughness on ground surfaces using speckle-contrast technique," Optics and Lasers in Engineering, **17**, No. 2, pp. 61-67.

[18] Asakura, T., 1978, "Surface roughness measurement," *Speckle Metrology*, edited by Erf, R.K., Academic Press, New York.

[19] Fujii, H., and Asakura, T., 1974, "Effect of surface roughness on the statistical distribution of image speckle intensity," Optics Communications, **11**, No. 1, pp. 35-38.

[20] Hecht, E., 1998, *Optics*, Addison Wesley Longman, Reading, MA.

[21] Ohmori, H., and Nakagawa, T., 1995, "Analysis of mirror surface generation of hard and brittle materials by ELID grinding with superfine grain metallic bond wheels," CIRP Annals – Manufacturing Technology, **44**, No. 1, pp. 287-290.

[22] Tonshoff, H.K., Karpuschewski, B., Hartmann, M., and Spengler, C., 1997, "Grinding-and-slicing techniques as an advanced technology for silicon wafer slicing," Mach. Sci. Technol., **1**, No. 1, pp. 33-47.

[23] Zhang, J.M., Sun, J.G., and Pei, Z.J., 2002, "Subsurface damage measurement in silicon wafers by laser scattering," Transactions of the North American Manufacturing Research Institution of SME, **30**, pp. 535-542, also SME Technical paper, MS02-173, Society of Manufacturing Engineers, Dearborn, MI.